Energy Dissipation Efficiency of Unbonded Post-Tensioned Precast Concrete Beam-Column Connections with Beam-End Dampers

15 WCEE
LISBOA 2012

T. Koshikawa, H. Kadowaki & M. Matsumora
Hokkaido University, Japan

SUMMARY:
This study investigates the energy dissipation efficiency of unbonded post-tensioned precast concrete beam-column connections with beam-end dampers. To facilitate the analysis, an iterative sectional procedure designed to predict the moment-rotation relationship of this type of connections is developed. The procedure used in this analytical model focuses on gap-opening behavior at the beam-column interface. The accuracy of the analytical procedure is illustrated by comparing its behavior with results of previous experiments on connections equipped with different types of beam-end dampers. Then results of an analytical parametric study that investigated the effects of variations in the damper details on the moment-rotation behavior of the connections are presented. Based on the results, an approximate equation is presented to evaluate the supplemental energy dissipation by the dampers. The results yielded using this equation compare well with the results of the analytical model.

Keywords: Post-tensioning, Energy dissipation, Connections, Precast/prestressed concrete, Sectional analysis

1. INTRODUCTION

Beam-column connections fabricated with unbonded post-tensioned precast concrete members perform well, and are suitable for seismic resistant frame structures because of their large self-centering capability and ability to undergo sizeable nonlinear lateral displacements without significant damage (e.g., Cheok and Lew 1993; Priestley and MacRea 1996). However, because there are gaps at the interface between the beams and columns that widen when subjected to seismic loadings and the small parts of the beams adjacent to the columns tend to suffer damage, this type of connection cannot dissipate large amounts of energy. In order to enhance the energy dissipation of such beam-column connections while retaining their restricted residual deformation characteristics, engineers have developed various external dampers. Such dampers are designed to dissipate energy during seismic loading and take advantage of gap-opening displacements between the beam and column members.

This paper discusses the energy dissipation efficiency of unbonded post-tensioned precast concrete beam-column connections with beam-end dampers that have been subjected to cyclic inelastic loading. To facilitate this study, an iterative sectional analysis procedure designed to predict the moment-rotation relationship exhibited by this type of connections is developed. This procedure, applied to this analytical model, focuses on the behavior of the gap at the beam-column interface. The analytical model incorporates the nonlinear behavior of concrete in compression at the beam ends, the nonlinear behavior of the prestressing tendons in tension, and the nonlinear behavior of the dampers.

In this paper, the accuracy of this analytical model is confirmed by comparing its behavior with results obtained from previous experiments on unbonded post-tensioned precast concrete beam-column connections equipped with different types of beam-end dampers. Following this, a parametric analysis of how variations in damper details affect the moment-rotation behavior of the connections is

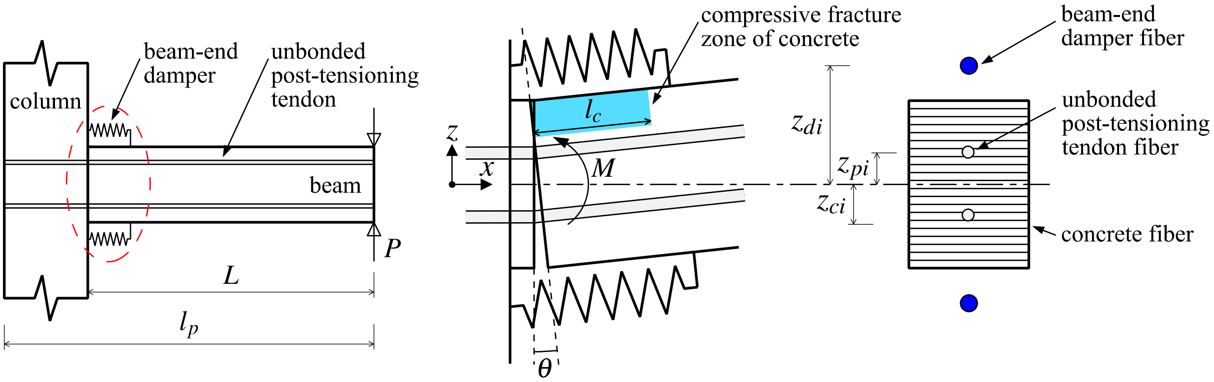

Layout of beam-column connection with beam-end dampers

Displaced configuration at beam-column interface

Beam-end cross section analytical model

Figure 2.1. Analytical model

presented. The main variables of the parametric study are the location of the beam-end dampers, the yield strength of the beam-end dampers, and the number of dampers.

2. ANALYTICAL MODEL

Nonlinear behavior of an unbonded post-tensioned precast concrete beam-column connection is mainly induced by the opening/closing of the gap at the beam-column interface. Structural damage in this type of connection under seismic loading occurs in the beam immediately adjacent to the column, with the remainder of the beam and the column remaining mostly elastic. Dampers, which provide energy dissipation for this connection, are placed in the beam-column joint region, connecting the beam and column. When the gap opens at the beam-column interface, it produces damper deformation (displacement). Thus, to accurately estimate the performance of this type of connection, it is necessary to have a realistic prediction of the moment-rotation relationship at the beam-column interface.

For the purpose of analysing the moment-rotation behavior at the beam-column interface of unbonded post-tensioned precast concrete beam-column connections with beam-end dampers, a sectional analysis procedure is presented. This procedure is iterative, arriving at results that satisfy the equilibrium of forces.

The analytical model for an exterior beam-column connection with beam-end dampers is shown in Fig. 2.1. The model assumes that the plane section on the beam-end moves axially and rotates rigidly, and displacement from the initial position occurs at the beam-column interface. The beam-end cross section is composed of a discrete number of concrete fibers and unbonded post-tensioning tendons. The beam-end damper fibers are also included in the analytical model. In the fiber analysis technique, each fiber is analysed individually while satisfying equilibrium conditions at the beam-end cross section. The way in which the beam end moment corresponding to a given rotation at the beam-column interface is calculated, based on the fiber analysis technique, is briefly described hereafter.

Using a given rotation θ and an assumed axial displacement u, which are defined at the x-axis through the beam centerline, the displacements in a concrete fiber u_{ci}, an unbonded post-tensioning tendon fiber u_{pi}, and a beam-end damper fiber u_{di} are given by

$$u_{ci} = u - z_{ci}\,\theta \tag{2.1}$$
$$u_{pi} = u - z_{pi}\,\theta \tag{2.2}$$
$$u_{di} = u - z_{di}\,\theta \tag{2.3}$$

where z_{ci}, z_{pi} and z_{di} are the distances from the x-axis of a concrete fiber, an unbonded post-tensioning tendon fiber and a beam-end damper fiber, respectively. The strain in a concrete fiber ε_{ci} is calculated by defining the length of the compressive fracture zone l_c, and the strain in an unbonded post-tensioning tendon fiber ε_{pi} is calculated by using the whole length of the tendon l_p. The deformation in a beam-end damper fiber d_{di} is assumed to be equal to the displacement u_{di}. These strains and the deformation are given by

$$\varepsilon_{ci} = \frac{u_{ci}}{l_c} + \overline{\varepsilon_{ci}} \tag{2.4}$$

$$\varepsilon_{pi} = \frac{u_{pi}}{l_p} + \overline{\varepsilon_{pi}} \tag{2.5}$$

$$d_{di} = u_{di} \tag{2.6}$$

where $\overline{\varepsilon_{ci}}$ and $\overline{\varepsilon_{pi}}$ are the initial strains due to post-tensioning in a concrete fiber and in an unbonded post-tensioning tendon fiber, respectively. The stresses in a concrete fiber σ_{ci} and in an unbonded post-tensioning tendon fiber σ_{pi} are calculated by using the stress-strain relationships for each of the components. The force in a beam-end damper fiber F_{di} is derived from the damper force-deformation relationship.

To check the equilibrium conditions, the normal force N at the beam-end cross section is calculated by summing the normal forces in each fiber as described below

$$N = \sum_i a_{ci}\, \sigma_{ci} + \sum_i a_{pi}\, \sigma_{pi} + \sum_i F_{di} \tag{2.7}$$

where a_{ci} and a_{pi} are the cross-sectional areas of a concrete fiber and an unbonded post-tensioning tendon fiber, respectively. The calculations of Eqns. 2.1 to 2.7 shown above are iterated until the equilibrium conditions of $N = 0$ are satisfied by updating the value of the assumed axial displacement u. The beam end moment M is derived as below once the equilibrium condition is satisfied.

$$M = \sum_i a_{ci}\, \sigma_{ci}\, z_{ci} + \sum_i a_{pi}\, \sigma_{pi}\, z_{pi} + \sum_i F_{di}\, z_{di} \tag{2.8}$$

Material nonlinearity for each component is expressed by uniaxial cyclic constitutive relationships. These relationships are illustrated in Fig. 2.2. For concrete, only the relationship on the compressive side is considered because of the gap that exists between the beam end and column face. The monotonic stress-strain relation of concrete is represented by a parabolic equation in the ascending range and a linear relation in the descending post-peak part that continues until the stress becomes zero. To avoid the size dependence problem due to strain softening, the compressive fracture energy G_{Fc} is introduced into the shaded area in the figure. For a post-tensioning tendon, the Menegotto-Pinto model is used for the monotonic and hysteretic stress-strain relationships. For a beam-end damper, the force-deformation relationship suited for the type of damper in each case is used.

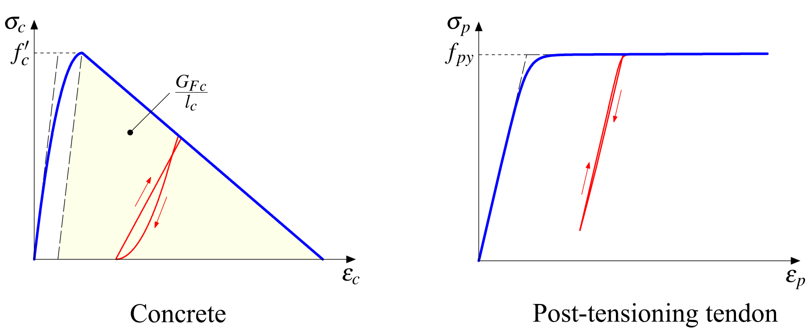

Figure 2.2. Uniaxial stress-strain relationships used in analytical model

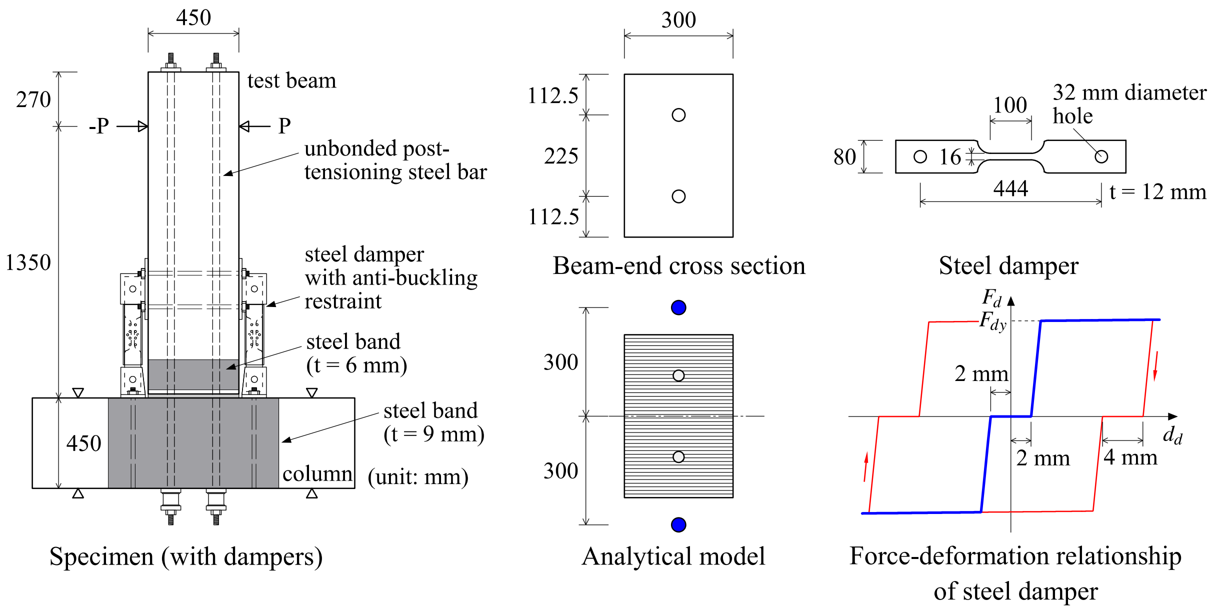

Figure 3.1. Test setup (Yano et al. 2010) and analytical model

3. EXPERIMENTAL VERIFICATION OF ANALYTICAL MODEL

To verify the accuracy of the proposed analytical procedure, two series of experimental results were selected. One is a series using beam-column connections with steel dampers (Yano et al. 2010), and the other is a series using connections with friction dampers (Morgen and Kurama 2004).

3.1. Beam-column Connections with Steel Dampers

Yano et al. (2010) tested a series of precast concrete beam-column connections with beam-end steel dampers. Two of these connections, specimens with and without dampers, are used for this study. The configuration of these specimens was the same except for the dampers. The specimen with dampers is shown in Fig. 3.1. The test beam, oriented in a vertical configuration, and the column were connected using two 23 mm diameter unbonded post-tensioning steel bars placed inside the beam and through the beam-column connections. Each post-tensioning steel bar was tensioned to a force of 270 kN, and the resulting axial compressive stress of 4 N/mm^2 was carried by the beam cross section. The column was designed not to deform. Steel dampers were placed parallel to the beam at the upper and lower sides of the beam face in the connection region, to utilise the displacement opening the gap opening at the beam-column interface and to provide energy dissipation by yielding in tension and in compression under cyclic loadings. A 32 mm diameter hole was drilled in each end of each damper. The dampers were attached to the beam and column through the steel brackets, inserting 30 mm diameter bolts through the holes in the brackets and dampers. Thus, clearances exist between the holes in the dampers and the surfaces of the bolts. To keep the dampers from buckling in compression, they were inserted into steel anti-buckling restraints. The dampers were initially stress-free since they were attached into the connections after the post-tensioning force was applied.

In the analytical models, the beam-end cross section is divided into 45 concrete fibers as shown in Fig. 3.1. The assumed material properties are as follows: For concrete, the compressive strength f_c' is 54 N/mm^2, the compressive fracture energy G_{Fc} is 120 N/mm, and the length of the compressive fracture zone l_c is 225 mm (half the beam depth). The yield strength f_{py} is 1093 N/mm^2 for the post-tensioning steel bar. For the force-deformation relationship of the steel dampers, the yield force is 83 kN, and a slip region of deformation is assumed when the force changes from tension to compression or from compression to tension, considering the clearance between the holes in the dampers and the surfaces of the bolts.

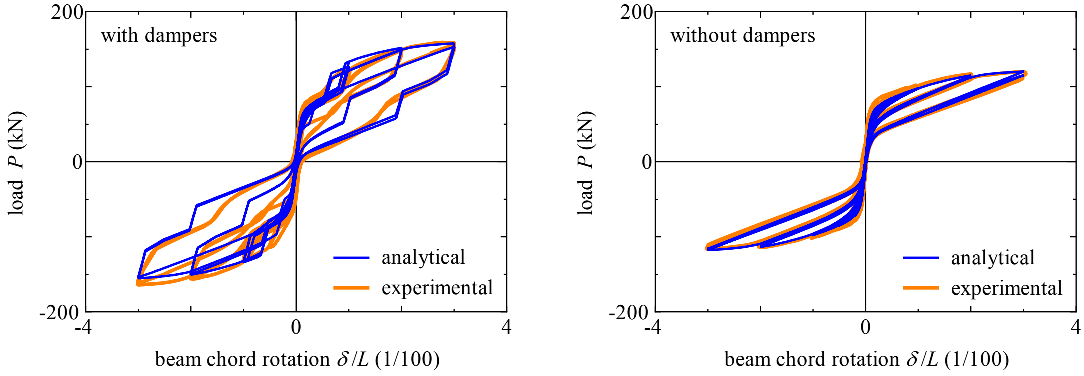

Figure 3.2. Comparison of load-beam chord rotation responses

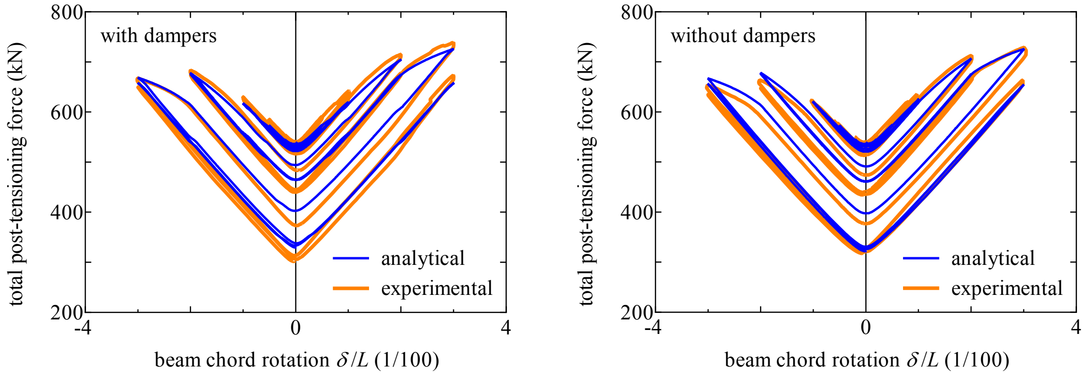

Figure 3.3. Comparison of total post-tensioning force-beam chord rotation responses

Fig. 3.2 compares the analytical responses with the test results for the load-beam chord rotation relationships of specimens with and without dampers. In calculating the beam chord rotation in the analytical models, the contribution to the deflection of the beam's elastic flexural deformation is considered together with that of the rotation at the beam-column interface. The analytical responses agree closely with the test results, including the differences in the specimens' behavior with and without dampers. Another comparison between the analytical model and test results for the total post-tensioning force-beam chord rotation relationship is shown in Fig. 3.3. The post-tensioning force was measured during the test with load cells positioned at the end of the post-tensioning steel bars. The analytically modeled responses of the overall variation of the total post-tensioning force with beam chord rotation are in good agreement with the test results.

3.2. Beam-column Connections with Friction Dampers

Morgen and Kurama (2004) tested a series of unbonded post-tensioned precast concrete beam-column connections with beam-end friction dampers. Two different specimens, referred to as Test 47 and Test 49, are used in this study. The experimental setup is shown in Fig. 3.4. The basic configuration of these specimens was similar to that considered in the previous section except for the location of the post-tensioning tendons and the type of dampers. In order to prevent yielding of the post-tensioning tendons and maintain the clumping force at higher rotation levels, the post-tensioning tendons were placed at the centerline of the beam. Each tendon comprised seven strands with a diameter of 15.2 mm, and was tensioned to a force of approximately 630 kN. The dampers used in these specimens utilised friction forces brought by slip displacements at the friction surfaces when the gaps open at the beam-column interfaces. The dampers had four friction surfaces in between the damper components, connected to the beam and to the column. The friction surfaces were clamped together using a damper normal bolt and disc spring washers to produce friction forces. The main difference between these specimens was the normal force $F_{dn,}$ carried by the damper, applied by the damper normal bolt. For

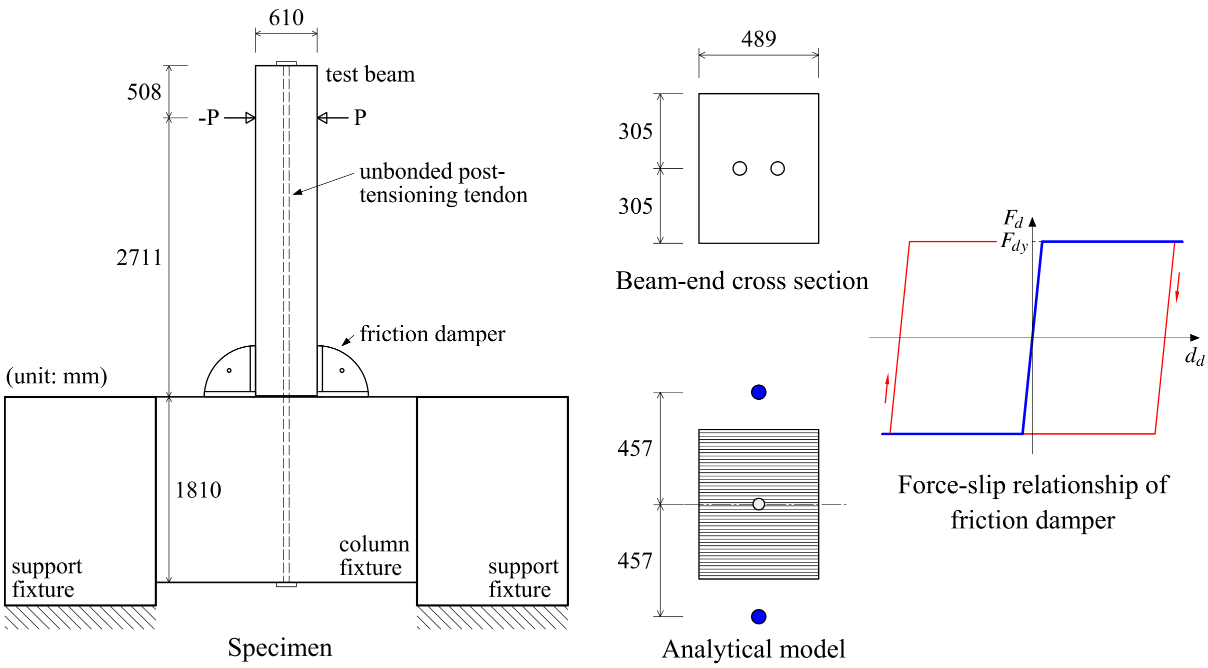

Figure 3.4. Test setup (Morgen and Kurama 2004) and analytical model

Test 47, a damper normal force of 116 kN was applied, while for Test 49, a damper normal force of 231 kN was applied. Note that the same test beam was reused through this series of test.

In the analytical models, the beam-end cross section is divided into 45 concrete fibers as shown in Fig. 3.4. Each friction damper is assumed to be 457 mm from the beam's centerline. The force-slip relationship of the friction damper is modeled as showing elastic-perfectly plastic hysteretic behavior. The yield force for the friction damper is calculated as the damper normal force multiplied by the number of friction surfaces times the coefficient of friction (Morgen and Kurama 2009). Other material properties used in the models are: For concrete, the compressive strength f_c' is 71 N/mm^2, the compressive fracture energy G_{Fc} is 160 N/mm and the length of the compressive fracture zone l_c is 305 mm (half of the beam depth). The yield strength f_{py} of the post-tensioning tendon is 1103 N/mm^2.

The analytically modeled beam end moment-beam chord rotation responses are compared with physical test results in Fig. 3.5. There was a slight overestimation of the beam end moment in Test 47, and an underestimation of the beam end moment in Test 49. These differences most likely resulted from where each friction damper was assumed to be located in the analytical models. However, the analytical models estimate the tendency of the test results relatively well.

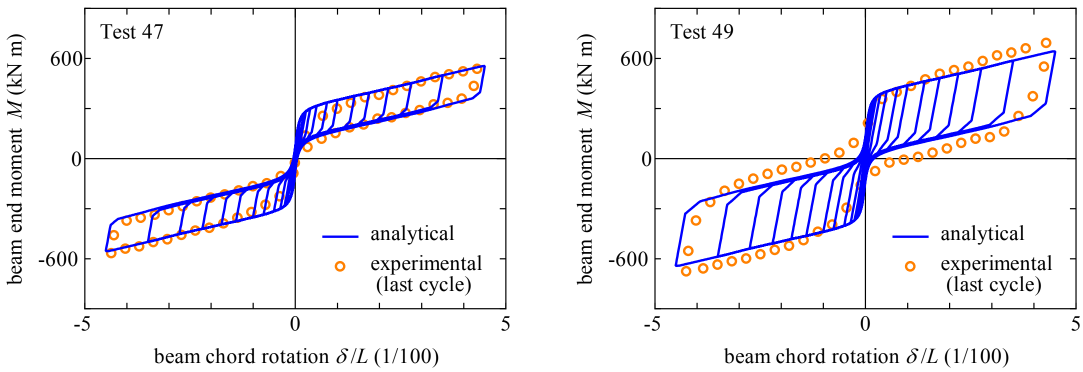

Figure 3.5. Comparison of beam end moment-beam chord rotation responses

4. PARAMETRIC STUDY

The conceptual moment-rotation response developed at the beam-column interface of unbonded post-tensioned precast concrete beam-column connections with beam-end dampers is a combination of the contributions made by the post-tensioning tendons and the beam-end dampers. The hysteretic behavior provided by the post-tensioning tendons exhibits an essentially nonlinear elastic response, with little energy dissipation. The beam-end dampers dissipate most of the energy in these connections. Therefore, the energy dissipation efficiency of these connections can be obtained from the contribution of the beam-end dampers on the moment-rotation response.

To investigate the effects of damper detail variations on energy dissipation efficiency, a parametric study of the analytical model of the Test 47 specimen configuration was performed. The parameters of interest were the damper yield force F_{dy}, the distance of the damper from the beam centerline z_d and the number of dampers n. Three damper yield forces (F_{dy} = 100, 200 and 300 kN), three distances from the beam centerline, based on the beam depth D (z_d / D = 0.5, 0.75, 1.0), and two sets of dampers (n = 1 and n = 2) were used. For n = 2, it was assumed that dampers having the same yield force were arranged symmetrically about the beam centerline in the same way as in the test specimen. For n = 1, it was assumed that the damper is placed under the beam only.

Examples of analytically modeled behavior in Fig. 4.1 illustrate the beam end moment-rotation responses modeled for n = 1 and 2, for beam-column connections with damper(s) having F_{dy} = 200 kN and z_d/D = 0.75. The contribution of the beam-end damper(s) to the moment-rotation response can be calculated by subtracting the moment derived by analyzing a beam-column connection without dampers from that shown in Fig. 4.1 at the same rotation. The resulting damper contributions for a single cycle corresponding to rotation of ±0.04 rad in these cases are shown in Fig. 4.2. The responses for n = 2 are symmetric in each half loading cycle, but the responses are not symmetric for n = 1.

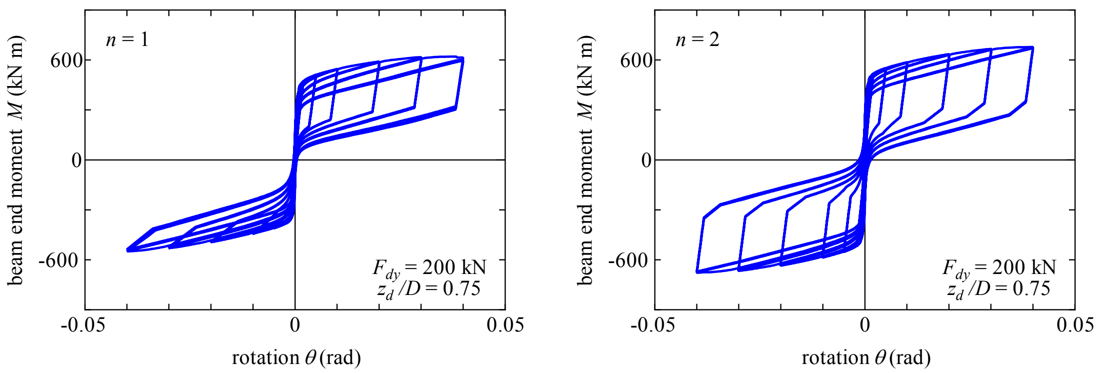

Figure 4.1. Modeled beam end moment-rotation response

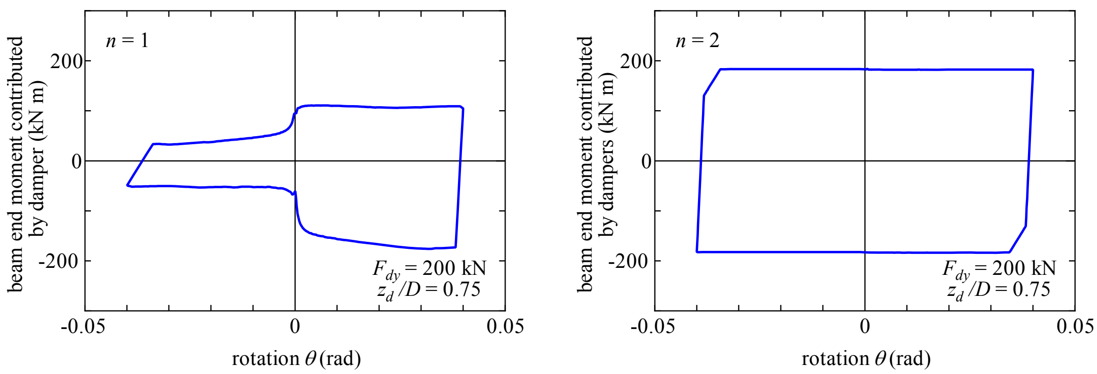

Figure 4.2. Damper contribution at $\theta = \pm 0.04$ rad

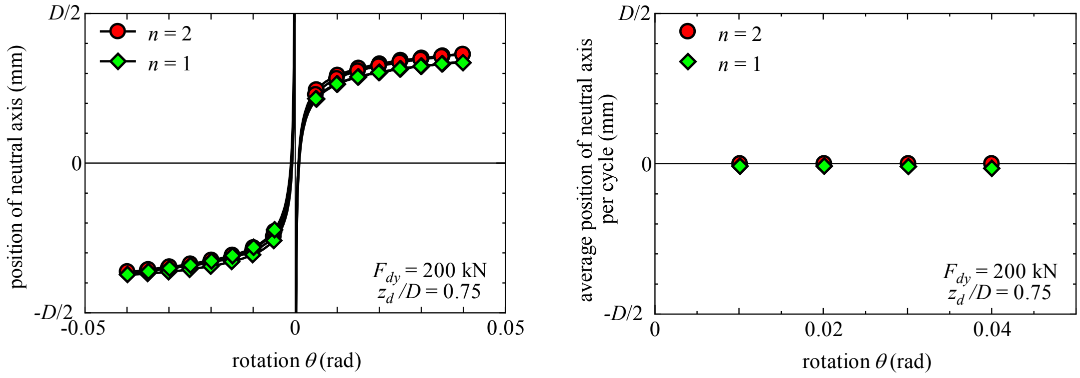

Figure 4.3. Position of neutral axis-rotation at $\theta = \pm 0.04$ rad and average position of neutral axis per cycle

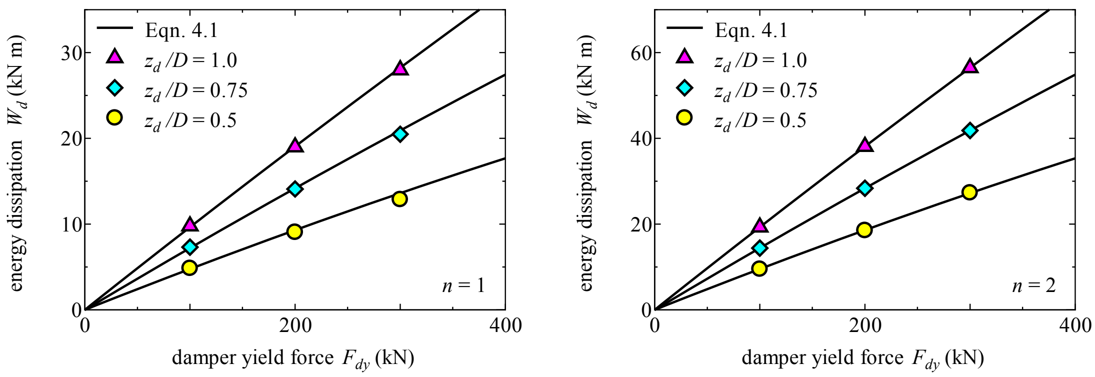

Figure 4.4. Comparison of supplemental energy dissipated per cycle by damper(s), at $\theta = \pm 0.04$ rad

The amount of supplemental energy dissipation provided by the damper(s) for a beam end moment-rotation cycle can be evaluated directly from the area enclosed by the hysteresis loop for that cycle as shown by the examples in Fig. 4.2. For $n = 2$, the energy dissipation W_d can be also estimated by the following equation for a target cycle of rotation θ because the shape of the hysteresis loop exhibits a cyclic response close to elastic-perfectly plastic behavior.

$$W_d = 4\,M_{dy}\left(\theta - \theta_y\right) \tag{4.1}$$

where M_{dy} = the equivalent moment contribution associated with the yield forces of the dampers. θ_y = the equivalent rotation associated with the yield deformation of the dampers. Although both M_{dy} and θ_y are related to the position of the neutral axis at which damper yielding begins, and the position of neutral axis varies during the cycle shown in Fig. 4.3, the average position of the neutral axis per cycle stabilizes on the beam centerline, as also shown in Fig. 4.3. For $n = 1$, the variation of the position of neutral axis is similar to the case where $n = 2$, and the average position of the neutral axis per cycle is almost on the beam centerline. Based on these results, M_{dy} and θ_y to be

$$M_{dy} = n\,z_d\,F_{dy} \tag{4.2}$$

$$\theta_y = \frac{F_{dy}}{z_d\,E_d} \tag{4.3}$$

where E_d = the elastic axial stiffness of the damper, in order to calculate W_d in Eqn. 4.1.

Fig. 4.4 compares the estimates from Eqn. 4.1 with the analytical results for the amount of supplemental energy dissipated per cycle provided by the damper(s), corresponding to a rotation of ±0.04 rad in each case. The analytical results indicate that the energy dissipation increases linearly with the increase of both the damper yield force F_{dy} and the distance of the damper from the beam centerline z_d / D. The estimates are in good agreement with the analytical results regardless of the number of dampers n.

5. CONCLUSIONS

The energy dissipation efficiency of unbonded post-tensioned precast concrete beam-column connections with beam-end dampers was investigated analytically. The analytical models used in this paper are based on a nonlinear sectional analysis procedure designed to predict the moment-rotation relationship at the beam-column interface of this type of connections. The comparison of analytical and experimental results has demonstrated that the analytical models perform well in terms of hysteretic behavior and energy dissipation. The results of an analytical parametric study that investigated the effects of variations in the damper details on the moment-rotation behavior of the connections indicated that energy dissipation increases linearly with the increase of both the damper yield force and the distance of the damper from the beam centerline, and the approximate equation presented to evaluate the supplemental energy dissipated by the dampers estimates the results of the analytical model well.

ACKNOWLEDGEMENT
Part of this work was supported by JSPS KAKENHI (23760514).

REFERENCES

Cheok, G. and Lew, H. (1993). Model precast concrete beam-to-column connections subjected to cyclic loading. *PCI Journal.* **38:4**, 80-92.

Morgen, B. and Kurama, Y. (2004). A friction damper for post-tensioned precast concrete moment frames. *PCI Journal.* **49:4**, 112-133.

Morgen, B. and Kurama, Y. (2009). Characterization of two friction interfaces for use in seismic damper applications. *Materials and Structures.* **42:1**, 35-49.

Priestley, M. and MacRea, G. (1996). Seismic tests of precast beam-to-column joint subassemblages with unbonded tendons. *PCI Journal.* **41:1**, 64-81.

Yano, T., Koshikawa, T., Mizoguchi, M., Yamashita, H. and Ueda, M. (2010). Structural performance of unbonded post-tensioned beam-column connections with damper. *AIJ Journal of Technology and Design.* **16:32**, 145-150. (In Japanese)